Name of Journal: *Radiology Innovation*
Manuscript Type: Original Article

Study on intraoperative ultrasonographic features of small lung cancer lesions with ground glass nodules on computerized tomography

Short title: Study on intraoperative ultrasonographic features of lung cancer lesions with ground glass nodules

Zhe Chen[1#], Dongman Ye[1#], Fuzhi Pan[1#], Congxuan Zhao[2], Yiru Hou[1], Yan Yan[1], Tao Yu[1*]

[1]Department of Medical Imaging, Cancer Hospital of China Medical University, Liaoning Cancer Hospital & Institute, Shenyang 110042, Liaoning Province, China
[2]Department of Ultrasound, Affiliated Hospital of Liaoning University of Traditional Chinese Medicine, Shenyang 110033, Liaoning Province, China

[*]Corresponding author: Tao Yu, PhD, Department of Medical Imaging, Cancer Hospital of China Medical University, Liaoning Cancer Hospital & Institute, No.44 Xiaoheyan Road, Dadong District, Shenyang 110042, Liaoning Province, China
Email: yutao@cancerhosp-ln-cmu.com

ABSTRACT

Objective: This study intends to compare the preoperative high resolution computed tomography (HRCT) and intraoperative ultrasonic (partial contrast-enhanced ultrasonic) images of a group of small lung cancer lesions with ground glass nodules (GGN) on computerized tomography (CT), and to explore the imaging features of small lung cancer lesions with GGN and the sonographic findings of some GGN contrast-enhanced ultrasonic (CEUS).

Methods: 41 patients with CT with ground glass nodules confirmed by pathology in Cancer Hospital of China Medical University from January 2019 to December 2021 were collected. Among them, 15 patients were examined by intraoperative contrast-enhanced ultrasonic. All patients were examined by high resolution computed tomography (HRCT) before operation and intraoperative ultrasonic during video-assisted thoracoscopic surgery (VATS). SPSS 22.0 software was adopted for data processing. If the data were in accordance with normal distribution, t-test was adopted between groups, and Fisher exact probability test was adopted for univariate analysis. $P < 0.05$ suggested that the difference was statistically significant.

Results: (1) There was significant difference between pure ground glass nodule (pGGN) and partial ground glass nodule (mGGN) in nodule diameter, shape, marginal spiculation sign, lobulation sign, pleural traction or indentation sign. There was significant difference in the edge of nodules and the short diameter of lesions between pGGN and mGGN ($P < 0.05$). (2) There was significant difference in nodule size between preoperative HRCT and intraoperative ultrasonic ($P < 0.05$). There was a significant difference in the size of GGN between preoperative HRCT and intraoperative ultrasonic ($P < 0.05$). There was significant difference in the time to start enhancement (TE) and the time to peak (TTP) between GGN contrast-enhanced ultrasonic and collapsed lung tissue ($P < 0.05$). Among the 15 cases of CEUS, 13 cases of GGN showed “slow in and fast out” mode compared with collapsed lung tissue, and 2 cases of GGN showed “fast in and fast out” mode compared with collapsed lung tissue.

Conclusion: (1) In VATS operation of GGN lung cancer, the lesions observed by ultrasonic can be distinguished according to the shape and edge characteristics of the lesions on CT before operation. (2) In terms of intraoperative ultrasonographic features of VATS, mGGN has a longer short diameter of lesions than pGGN, and the edge of lesions is more lobulated. (3) Contrast-enhanced ultrasonic mostly showed low enhancement in GGN micro-lung cancer, and its contrast-enhanced mode was “slow in

and fast out”. The use of this feature is beneficial to the confirmation of micro-lung cancer nodules during operation.

Keywords: Intraoperative ultrasonic; Ground glass nodules of the lung; Contrast-enhanced ultrasonic; Video-assisted thoracoscopic surgery

INTRODUCTION

Lung cancer is one of the malignant tumors with the highest morbidity and mortality in the world,[1] and surgical resection is the main treatment. Pulmonary nodules were defined as smaller than 3cm in diameter, round or irregular in shape, regular or irregular boundary, single or multiple nodules, and high density shadow on imaging findings.[2] It is generally believed that the larger the diameter of the nodule, the higher the risk of malignancy. Micro lung cancer refers to carcinoma in situ and stage I lung cancer.[3] The early diagnosis of micro lung cancer is very important. Studies have shown that the 5-year survival rate of patients with stage I non-small cell lung cancer is about 80%, and that of patients with stage II–III non-small cell lung cancer is about 13%–60%.[4] With the increasing awareness of physical examination and the widespread acceptance of low-dose computed tomography (LDCT) and high resolution computed tomography (HRCT) of the chest, more and more small nodules and small lung cancer are detected as early as possible for screening, and then get surgical treatment.

In recent years, with the continuous innovation and progress of thoracic surgery technology, video-assisted thoracoscopic surgery (VATS) has been adopted in thoracic surgery. Because it can effectively shorten the length of stay, reduce postoperative complications and shorten the time of chest tube drainage, it has gradually replaced the traditional thoracotomy and become the routine treatment of small pulmonary nodules. However, in VATS surgery, for small and deep subpleural nodules, the location of nodules cannot be determined by visual examination, palpation, or instrument sliding. During the operation, it is inevitable to expand the scope of resection, convert to thoracotomy or re-perform intraoperative computerized tomography (CT) localization due to the failure to locate the nodules accurately. As reported in the early literature, the probability of switching to thoracotomy without accurate location of nodules is about 46%.[6] Although the localization ability of pulmonary nodules during operation has been greatly improved with the progress of technology, it is still difficult to locate ground glass nodules (GGN) with few solid components and soft texture, which to a certain extent leads to the increase of operation time, the difficulty of operation and the prolongation of anesthesia time, which brings some risks to patients.[7.8] As a consequence, how to find nodules efficiently, locate nodules accurately and effectively reduce the conversion rate of thoracotomy has become one of the urgent problems for clinicians.

At present, there are many ways to locate pulmonary nodules, including preoperative and intraoperative localization. Preoperative localization methods include percutaneous injection of dyes (such as methylene blue, lipiodol, *etc*.), percutaneous hook wire localization guided by CT, percutaneous coil localization under the guidance of CT, etc., which provide a good visual guidance for the operation. However, these invasive localization methods all have possible complications such as wound bleeding, postoperative puncture point pain and so on. Hook wire or coil positioning may also have the risk of falling off, pneumothorax and hemothorax.[9] Because dye diffusion speed is too fast, it can result in excessive location of the lung surface, which often leads to the expansion of the scope of pneumonectomy; lipiodol localization often leads to allergic reactions in patients, and even leads to the occurrence of anaphylactic shock. In recent years, intraoperative ultrasonic has been gradually applied to the intraoperative localization of pulmonary nodules because of its advantages of non-invasive, simple and repeatable, and has been proved to be a simple and safe method for visualization of intraoperative pulmonary nodules.[10–12] Huang,[13] Hou[14] and other scholars have studied the detection of pulmonary nodules by intraoperative ultrasonic. The results show that the success rates of intraoperative ultrasonic localization in pure ground glass nodules (pGGN) group and partial ground glass nodule (mGGN) group are 90% and 100%, respectively. Intraoperative ultrasonic can locate tiny pulmonary nodules that can not be found by visual examination and palpation without damaging the pulmonary parenchyma. But up to now, the study of ultrasonographic features of small lung cancer lesions with GGN on CT is still rare, and the summary of contrast-enhanced ultrasonographic features has not been reported.

Based on this, this study uses intraoperative ultrasonic to scan the lesions of small lung cancer with GGN on CT, and to summarize the imaging features of two-dimensional ultrasonic and contrast-enhanced ultrasonic in vats, so as to provide a basis for the diagnosis and differentiation of micro-lung cancer with GGN on CT.

MATERIALS AND METHODS

Objects

A total of 41 patients with "ground glass nodules" diagnosed by CT in Cancer Hospital of China Medical University and confirmed by operation and pathology were collected, including 9 males and 32 females, aged from 40 to 78 years, with an average age of 60.10 years. High resolution chest CT was performed within two weeks before operation, and intraoperative ultrasonography was performed during operation. Among them, a total of 44 nodular lesions were detected. 44 ground glass nodules with small lung cancer were examined by ultrasonic, and 15 of them were also examined by contrast-enhanced ultrasonic after ultrasonic examination.

Inclusion criteria: (I) No previous history of malignant disease; (II) HRCT examination within two weeks before operation, which was diagnosed as “ground glass nodule” with a diameter smaller than 3cm and “high possibility of malignancy”; (III) The patient did not undergo biopsy, localization and other treatment before operation. (IV) Patients and their family members agreed to VATS operation and intraoperative ultrasonic examination (those who agreed with contrast-enhanced ultrasonic examination would be further examined by contrast-enhanced ultrasonic after the completion of color Doppler examination), and (V) Intraoperative ultrasonic could well display the lesions.

Exclusion criteria: (I) Patients with incomplete clinical data; (II) Patients who could not tolerate one-lung ventilation; (III) Patients or family members who did not agree to VATS surgery; (IV) Patients who were allergic to ultrasonic contrast agents; (V) Lack of stable vital signs during the operation were not suitable for intraoperative ultrasonic examination; (VI) Deep lesions and poor pulmonary collapse made it difficult to show the lesion clearly.

Imaging examination

Preoperative HRCT examination: Philips256iCT, CT scanning parameters: tube voltage 120 kVp, matrix 512, scan thickness 5mm and 1mm thin layer reconstruction. The HRCT was read by two or more doctors, and the shape, size, number, edge and location of GGN in the lung were observed and recorded.

Intraoperative ultrasonic examination: BK Pro lesion 2202 ultrasonic diagnostic instrument, the probe is BK laparoscopic probe, probe frequency is 5.5–10 MHz (probe diameter is 10mm, long 35cm, scanning angle is 60 degrees). Low temperature plasma method was adopted to disinfect the ultrasonic probe before operation. During VATS, general anesthesia was induced, double-lumen endotracheal intubation, contralateral one-lung ventilation, and the position of intubation was confirmed by fiberoptic bronchoscopy of unilateral lung ventilation. After the lung collapses, the nodules are initially marked by instrument sliding palpation. When the operative side of the lung reached the maximum collapse, the probe was placed on the surface of the lung through the surgical hole, and the probe was adopted to exert pressure on the pleura to partially empty the lung. the lesions were scanned from multiple angles on the surface of the lung, and the data were collected and recorded by ultrasonic doctors. The collected data include the shape and echo of the nodule, the maximum diameter, the boundary and so on.

Intraoperative contrast-enhanced ultrasonic examination: after the completion of intraoperative ultrasonic examination, contrast-enhanced ultrasonic examination was performed. Sonowei (Bracco, Italy produced sulfur hexafluoride microbubble injection) was adopted and the contrast agent 5ml was adopted for backup. Laparoscopic probe was selected, the frequency was 5.5–10MHz, and the mechanical index was 0.1–0.2. Combined with the intraoperative ultrasonic findings, the best section was selected to enter the contrast mode. After the injection of 2.2 ml sonovir contrast agent, the warm sterilized saline 5 ml was quickly pushed into the contrast medium. At the same time, the contrast procedure was started and timing began. Get the dynamic image for 1 minute and 30 seconds and save it to the instrument hard disk.

The contrast-enhanced ultrasonic images stored in the analysis instrument were independently analyzed by two or more ultrasonic doctors in the subnormal high school, and the enhancement intensity and enhancement mode of pulmonary nodules and surrounding collapsed lung tissue were judged with naked eyes. at the same time, the starting enhancement time and time to peak of pulmonary nodule and collapsed lung tissue were recorded. The two doctors reached an agreement when the results of the analysis were inconsistent. The enhancement intensity was divided into: (1) high enhancement: the enhancement intensity of nodules was higher than that of collapsed lung tissue; (2) equal enhancement: the enhancement intensity of nodules was similar to that of collapsed lung tissue; (3) low enhancement: the enhancement intensity of nodules was lower than that of collapsed lung tissue; no enhancement: no contrast medium filling in nodules. The enhancement mode is divided into: (1) the nodule begins to enhance: when the nodule begins to enhance earlier than the collapsed lung tissue, it is called “fast forward”, on the contrary, it is called “slow forward”; (2) the nodule begins to fade: the nodule begins to fade earlier than the collapsed tissue is called “fast out”; on the contrary, it is “slow out”.

Pathological examination

Under the guidance of ultrasonic, the nodules were marked and wedge resection with the edge of 2cm was performed. After operation, the specimens were sent to the pathology department for frozen section histopathological examination to confirm the accuracy of resection. The lung lobes were removed and frozen for examination, paraffin embedded, sectioned, stained and microscopically diagnosed as benign and malignant lesions. After operation, the lung tissue was examined, and the size, boundary and shape of the nodules were recorded, and the specimens were examined by pathologists.

Statistical analysis

In view of the tiny lung cancer lesions with ground glass nodules on CT, the shape and echo of nodules, the maximum diameter of nodules, the boundary of nodules and the enhancement time, intensity and mode of contrast-enhanced ultrasonic were analyzed. Statistical Package for the Social Sciences (SPSS) 22.0 (IBM Corp., Armonk, NY, USA) was adopted for data processing. If it accorded with normal distribution, it was expressed by mean ± standard deviation ($M \pm SD$), t-test was adopted between groups, counting data was expressed by n or percentage, and Fisher exact probability test was adopted for univariate analysis. $P < 0.05$ suggested that the difference was statistically significant.

RESULTS

General information

A total of 44 nodules were resected in 41 cases, of which invasive adenocarcinoma accounted for 64%. According to the Union for International Cancer Control (UICC) / American Joint Committee on Cancer (AJCC) (eighth edition) Tumor Node Metastasis (TNM) staging standard of lung cancer, all cases were in the early stage. Most of the lesions were located in the upper lobe of the right lung. The imaging and pathological features of microlung cancer with ground glass nodules in this group (Supplementary Table 1). Ultrasonographic findings during VATS (Figure 1).

Supplementary Table 1. Imaging and pathological features of microlung cancer with ground glass nodules in this group.

Imaging and pathological features of nodules	Number of cases	Percentage
Nodular types in CT images		

Pure ground glass nodules	15	34%
Partially solid ground glass nodules	29	66%
Pathological classification		
Invasive adenocarcinoma	28	64%
Microinvasive adenocarcinoma	9	21%
Carcinoma in situ	6	13%
Mixed mucinous carcinoma	1	2%
TNM stage		
TisN0M0	6	13%
T1miN0M0	9	21%
T1aN0M0	2	4%
T1bN0M0	20	46%
T1cN0M0	7	16%
Lesion location		
Upper lobe of right lung	18	41%
Middle lobe of right lung	6	13%
Lower lobe of right lung	7	16%
Upper lobe of left lung	10	23%
Lower lobe of left lung	3	7%

CT: computerized tomography; TNM: Tumor Node Metastasis.

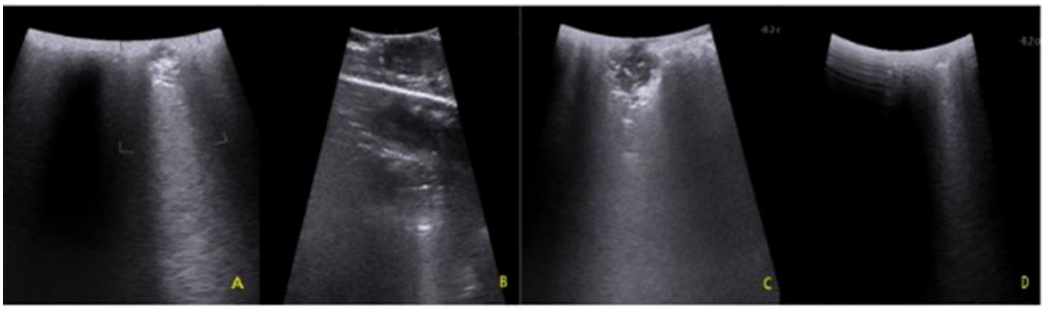

Figure 1. VATS intraoperative two-dimensional ultrasonographic images of microlung cancer with different pathological types of ground glass nodules. A. The intraoperative two-dimensional ultrasonic images of adenocarcinoma in situ in the upper lobe of the right lung by VATS showed that the size of the lesion was about 7.2 × 6.1 mm, with

inhomogeneous mixed echo inside, regular shape, clear boundary, no obvious lobulation and posterior echo enhancement. B. The intraoperative two-dimensional ultrasonic images of microinvasive adenocarcinoma in the left lower lobe of the lung were as follows: the size of the lesion was about 20.7 × 8.5 mm, the interior was uniform and hypoechoic, the shape was regular, the boundary was clear, shallow lobulation and slight enhancement of posterior echo could be seen. C. The intraoperative two-dimensional ultrasonic images of infiltrating adenocarcinoma in the lower lobe of the right lung showed that the size of the lesion was about 13.3 × 14 mm, with inhomogeneous echo, mainly hypoechoic, irregular shape, unclear boundary, lobulation and posterior echo enhancement. D. The intraoperative two-dimensional ultrasonic images of mixed mucinous carcinoma in the upper lobe of the right lung showed that the size of the lesion was about 7.4 × 8 mm, the internal echo was uniform, the internal echo was low, the shape was regular, the boundary was clear, there was no obvious lobulation, and the posterior echo was slightly enhanced. VATS: video-assisted thoracoscopic surgery.

HRCT and intraoperative ultrasonographic findings of small lung cancer with ground glass nodules of the lung

On HRCT images, there were significant differences in lesion diameter, lesion shape, lesion edge, edge lobulation and pleural changes between pGGN and mGGN ($P < 0.05$) (Table 1, Figure 2). In intraoperative ultrasonography, there was significant difference in lesion edge and short diameter between pGGN and mGGN ($P < 0.05$), but there was no significant difference in lesion shape, echo uniformity and echo type ($P > 0.05$) (Table 2, Figure 3). By comparing the preoperative HRCT images and intraoperative ultrasonic images of ground glass nodules, it was found that there was significant difference in the short diameter of the lesions measured by the two methods ($P < 0.05$), but there was no significant difference in the shape and edge of the lesions on preoperative HRCT images and intraoperative ultrasonic images ($P > 0.05$) (Table 3).

Table 1. CT imaging findings of micro-lung cancer with ground glass nodules

HRCT Performance	Pure ground glass nodules (n = 15)	Partially solid ground glass nodules (n = 29)	P Value

Lesion diameter	11.20 ± 3.96	16.93 ± 5.40	＜0.01[a]
Lesion shape			
Circle / quasi-circle	11	5	＜0.01[b]
Irregularity	4	24	
Edge of Lesion			
Smooth	13	1	＜0.01[b]
Burr sign	2	28	
Marginal lobulation			
Lobulation	1	20	＜0.01[b]
No lobulation	14	9	
Pleural changes			
Pleural indentation or traction	1	24	＜0.01[b]
No pleural depression	14	5	

[a]Independent sample *t*-test; [b]Fisher exact test. HRCT: high resolution computed tomography.

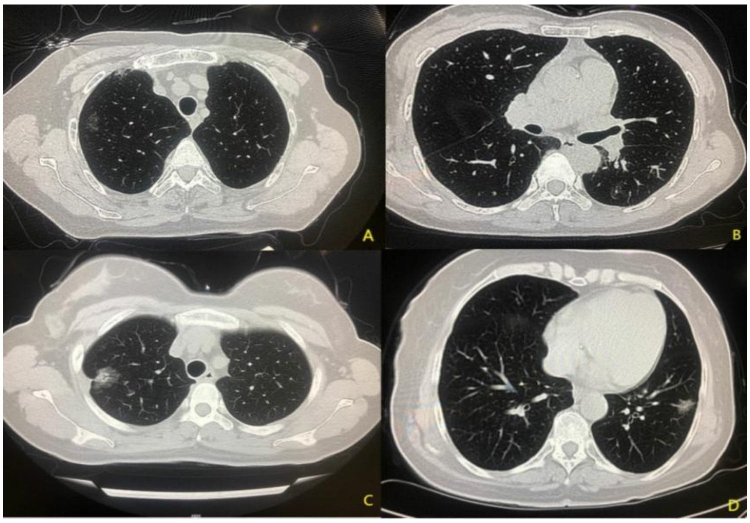

Figure 2. HRCT imaging findings of small lung cancer with ground glass nodules. A. Before operation, HRCT showed pure ground glass nodules in the upper lobe of the right lung: the size of the lesion was about 10 × 17 mm, with a density of pure ground glass nodules, regular shape, clear boundary, no lobulation, no signs of pleural traction or indentation. The pathology after operation was invasive adenocarcinoma. B. HRCT

showed pure ground glass nodules in the upper lobe of the left lung before operation: the size of the lesion was about 14 × 8 mm, with a density of pure ground glass nodules, regular shape, clear boundary, no lobulation, no signs of pleural traction or depression. Postoperative pathology was adenocarcinoma in situ. C. Before operation, HRCT showed partial solid ground glass nodules in the upper lobe of the right lung: the size of the lesion was about 28 × 25 mm, with partial solid ground glass nodules density, irregular shape, boundary spiculation changes, shallow lobulation signs, pleural traction or depression signs. Postoperative pathology was invasive adenocarcinoma. D. Before operation, HRCT showed partial solid ground glass nodules in the lower lobe of the left lung: the size of the lesion was about 20 × 15 mm, the density of partially ground glass nodules was irregular, the boundary was spiny, there were shallow lobulation signs, pleural traction or depression signs could be seen, and the postoperative pathology was slightly invasive adenocarcinoma. HRCT: high resolution computed tomography.

Table 2. Intraoperative ultrasonographic findings of small lung cancer with ground glass nodules in this group.

HRCT Performance	Pure ground glass nodules (n = 15)	Partially solid ground glass nodules (n = 29)	P Value
Lesion diameter	10.00 ± 4.09	13.38 ± 5.66	0.029[a]
Lesion shape			
Regularity	9	13	0.526[b]
Irregularity	6	16	
Edge of Lesion			
Clear	11	10	0.025[b]
Fuzzy	4	19	
Echo uniformity			
Uniform	10	14	0.342[b]
Non-uniform	5	15	
Echo type			
Low echo	11	21	1[b]
High echo	4	8	

[a]Independent sample t-test; [b]Fisher exact test. HRCT: high resolution computed tomography.

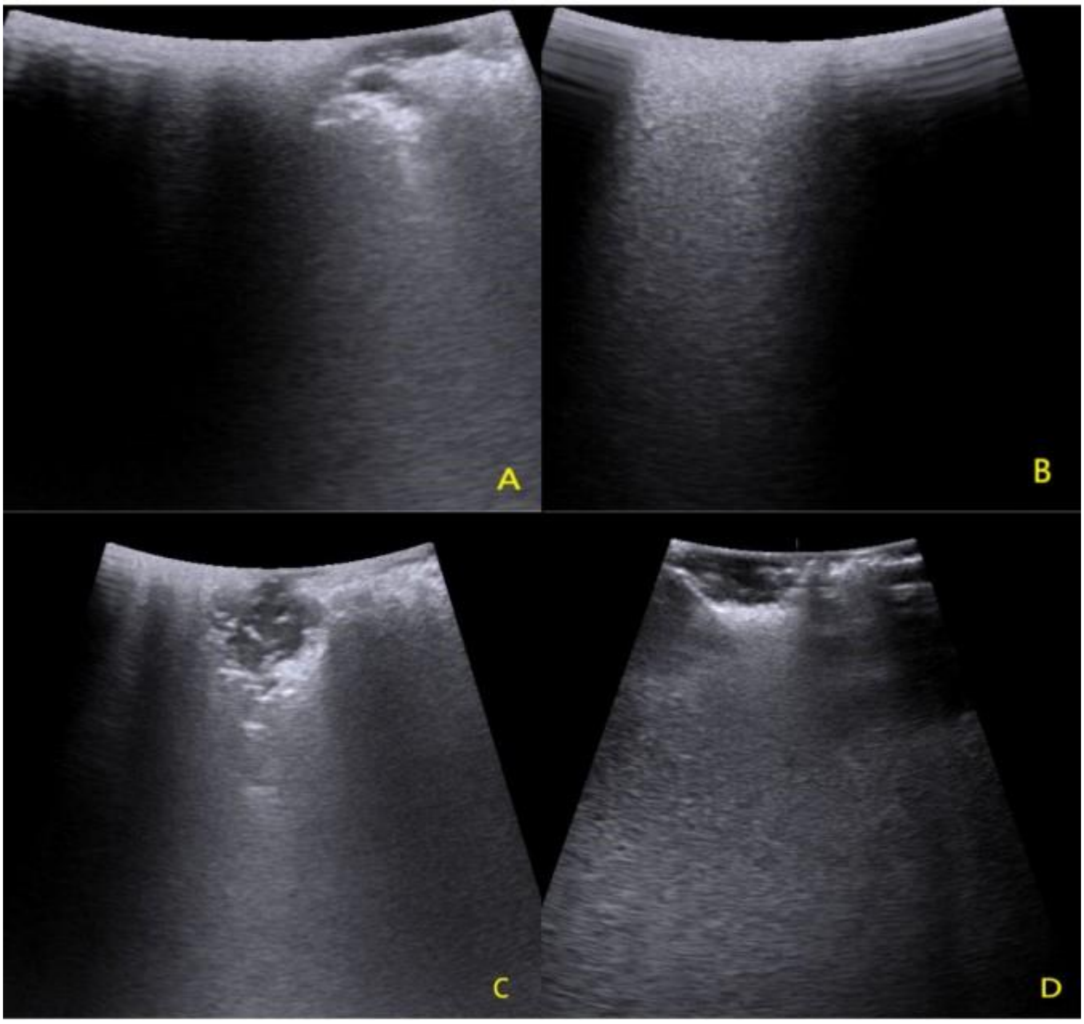

Figure 3. Intraoperative ultrasonographic findings of microlung cancer with ground glass nodules. A. Preoperative HRCT showed pure ground glass nodules in the upper lobe of the left lung. The intraoperative ultrasonic images of VATS showed that the size of the lesion was about 6.2 × 15.4 mm, the interior was uniform and hypoechoic, the shape was irregular, the boundary was clear, there was no obvious lobulation, and the posterior echo was not enhanced. The pathology after operation was invasive adenocarcinoma. B. preoperative HRCT showed pure ground glass nodules in the upper lobe of the left lung. Intraoperative ultrasonic images of vats showed that the size of the lesions was about 4.76 × 10.0 mm, the interior was uniform and hypoechoic, the boundary was still clear, there was no obvious lobulation, and the posterior echo was not enhanced. Postoperative pathology was adenocarcinoma in situ. C. preoperative HRCT showed partial solid ground glass nodules in the lower lobe of the right lung. The intraoperative ultrasonic images of vats showed that the size of the lesions was about 12.0 × 14.0 mm, and the interior showed inhomogeneous low echo. The shape is

irregular, the boundary is not clear, lobulation can be seen, the posterior echo is enhanced, and the postoperative pathology is invasive adenocarcinoma. D. The intraoperative HRCT images of solid ground glass nodules in the lower lobe of the right lung showed that the size of the lesion was about 8.0 × 12.0 mm, the interior was uniform and hypoechoic, the shape was regular, the boundary was still clear, there was no obvious lobulation, and the posterior echo was slightly enhanced. The pathology after operation was invasive adenocarcinoma. HRCT: high resolution computed tomography; VATS: video-assisted thoracoscopic surgery.

Table 3. Comparison of preoperative HRCT and vats intraoperative ultrasonographic findings of microlung cancer with ground glass nodules.

Nodular feature	Preoperative HRCT (n = 44)	Intraoperative ultrasonic (n = 44)	P value
Lesion diameter	14.98 ± 5.63	12.14 ± 5.45	$<0.01^a$
Lesion shape			
Regular / quasi-circular	16	22	0.282^b
Irregularity	28	22	
Edge of lesion			
Smooth / clear	14	21	0.191^b
Blurry / rough	30	23	

^{a}paired t-test; ^{b}Fisher exact test. HRCT: high resolution computed tomography.

Study on the characteristics of intraoperative contrast-enhanced ultrasonography in micro-lung cancer with ground glass nodules

Comparison of contrast-enhanced ultrasonographic parameters between small lung cancer lesions and collapsed lung tissues with ground glass nodules

A total of 15 ground glass nodules were examined by intraoperative contrast-enhanced ultrasonic (CEUS) in vats and compared with those of surrounding collapsed lung tissues. The mean time to enhancement (TE) and time to peak (TTP) of GGN contrast medium were 13.53 ± 3.58 s, 22.27 ± 3.86 s, and 7.00 ± 1.92 s, 12.60 ± 2.38 s, respectively. In this group, the intraoperative contrast-enhanced ultrasonic indexes of lung cancer and surrounding collapsed lung tissue in the early stage of ground glass nodule were compared (Table 4). There were significant differences between micro-lung cancer and surrounding collapsed lung tissue in TE and TTP ($P < 0.05$).

Table 4. Intraoperative contrast-enhanced ultrasonographic parameters of microlung cancer and surrounding collapsed lung tissue with ground glass nodules in this group

	TE	TTP
Ground glass nodule of lung	13.53 ± 3.58	22.27 ± 3.86
Surrounding collapsed lung tissue	7.00 ± 1.92	12.60 ± 2.38
t^a	5.16	7.34
P	0.00	0.00

[a]paired *t*-test. TE: time to enhancement; TTP: time to peak.

VATS contrast-enhanced ultrasonographic features of small lung cancer with ground glass nodules of the lung

A total of 15 ground glass nodules were examined by intraoperative contrast-enhanced ultrasonic in vats (Table 5). In the enhanced mode, 13 GGN showed a “slow in and fast out” pattern compared with the surrounding collapsed lung tissue (Figure 4 and Figure 5), and 2 GGN showed a “fast in and fast out” mode compared with the surrounding collapsed lung tissue (Figure 6). In terms of enhancement intensity, 12 GGN showed low enhancement (Figure 7), 1 GGN showed equal enhancement (Figure 8), and 2 GGN showed high enhancement (Figure 9). In terms of TE time, the TE of 3 GGN was between 6–10s, the TE of 12 GGN was greater than 10s, the TE of 5 collapsed lung tissues around nodules was between 0-6s, and the TE of 10 collapsed lung tissues was between 6–10s. Our team found that CEUS can well identify the difference between GGN and collapsed lung tissue during VATS.

Table 5. Contrast-enhanced ultrasonographic features of ground glass nodules

	Radiographic mode	Number of cases	Percentage
Enhancement mode	Slow in and fast out	13	87%
	Fast in and out.	2	13%
	Go in and out together	0	0
Enhancement strength	High enhancement	2	13%

Low enhancement	12	80%
Equal enhancement	1	7%
GGN start enhancement time		
0–6s	0	0
6–10s	3	20%
＞10s	12	80%
The time when the collapsed lung tissue begins to enhance.		
0–6s	5	33%
6–10s	10	67%
＞10s	0	0

GGN: ground glass nodules.

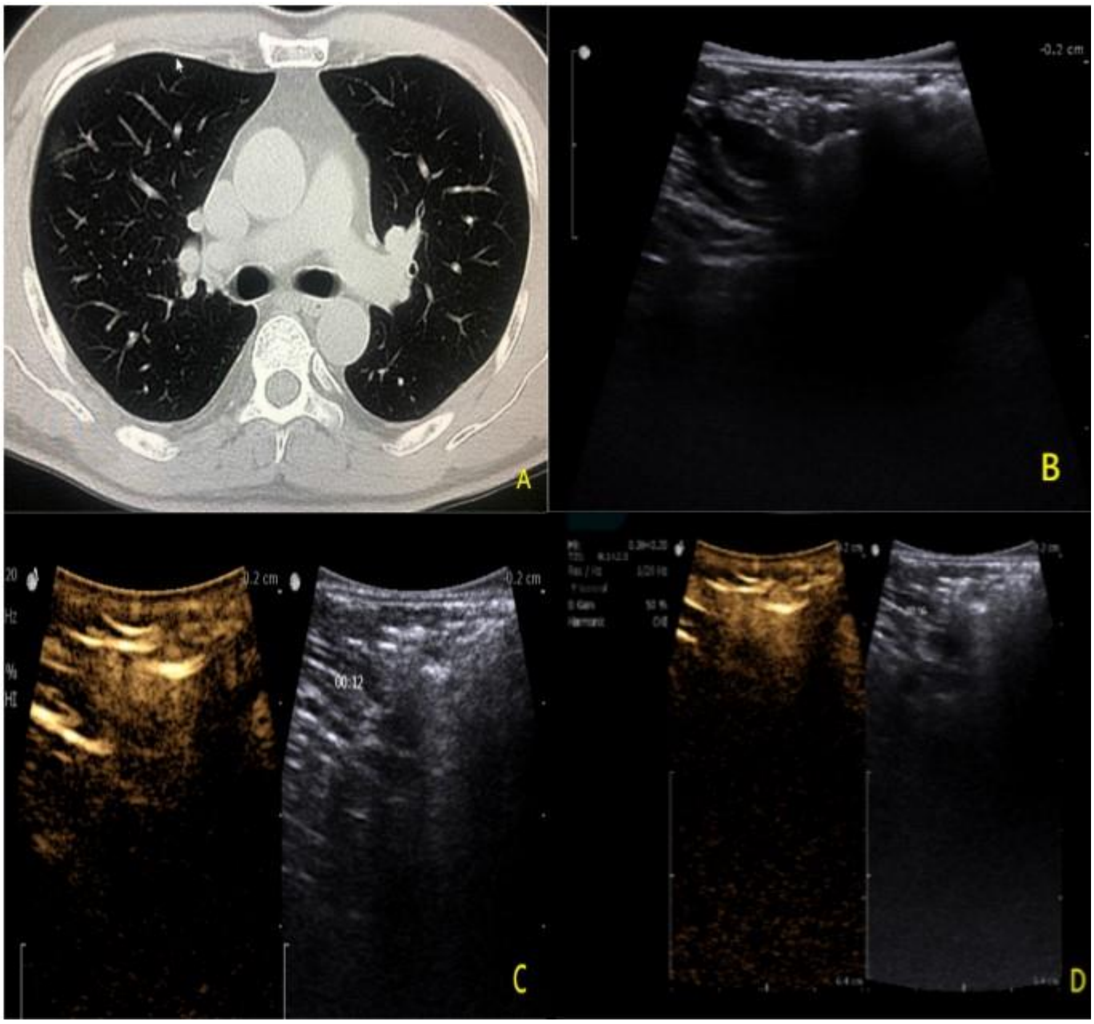

Figure 4. Image of preoperative HRCT, intraoperative two-dimensional ultrasonic and contrast-enhanced ultrasonic in patients with pGGN. A. Before operation, HRCT

showed pGGN density of 15mm in the anterior segment of the upper lobe of the right lung, with uniform density, regular shape, smooth edge, no lobulation and no burr-like changes. B: Intraoperative two-dimensional ultrasonic showed that the nodule showed mixed echo, regular shape, clear edge, no obvious lobulation and no obvious crab foot infiltration. C, D. Intraoperative CEUS showed that the nodule began to enhance in 12 seconds and reached the peak in 16 seconds; the nodular enhancement was mainly marginal enhancement, but the central enhancement was not obvious, and then disappeared rapidly, showing a “slow in and fast out” appearance. HRCT: high resolution computed tomography; pGGN: pure ground glass nodule; CEUS: contrast-enhanced ultrasonic.

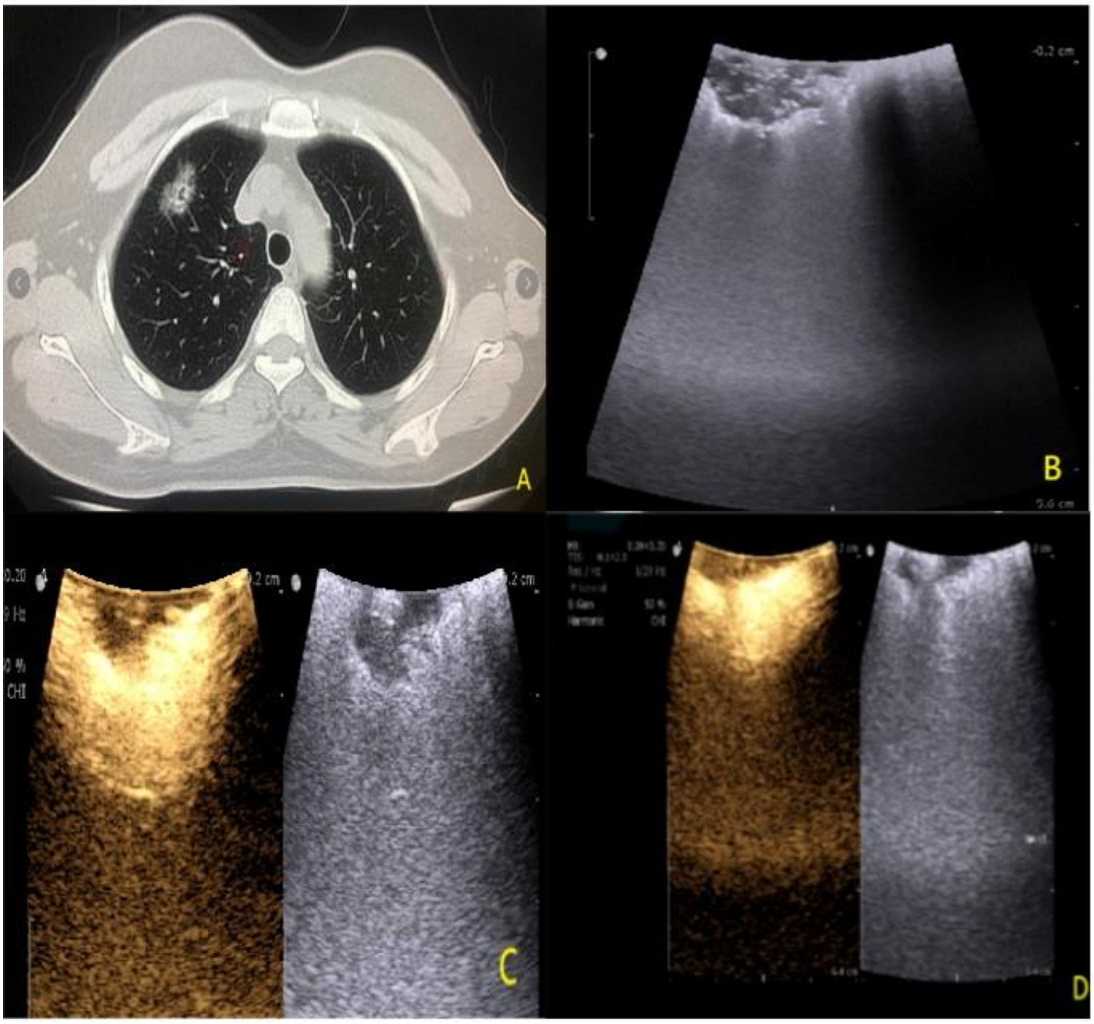

Figure 5. Characteristics of preoperative HRCT, intraoperative ultrasonic and contrast-enhanced ultrasonic in invasive adenocarcinoma. A. Before operation, HRCT showed mGGN density shadow of diameter 25mm in the anterior segment of the upper lobe of the right lung, the density was uneven, the shape was irregular, the edge showed burr-

like changes, shallow lobulated changes, traction close to the pleura, and the cavity could be seen inside. B. Intraoperative two-dimensional ultrasonic showed that the nodule showed low echo, unclear boundary, irregular shape and crab foot infiltration. C, D. Intraoperative CEUS showed that the nodules began to enhance in 12 seconds, and reached the peak in 18 seconds. The nodules enhanced mainly in the edge, but not in the center, and then disappeared rapidly, showing a “slow in and fast out” appearance. HRCT: high resolution computed tomography; CEUS: contrast-enhanced ultrasonic. mGGN: partial ground glass nodule.

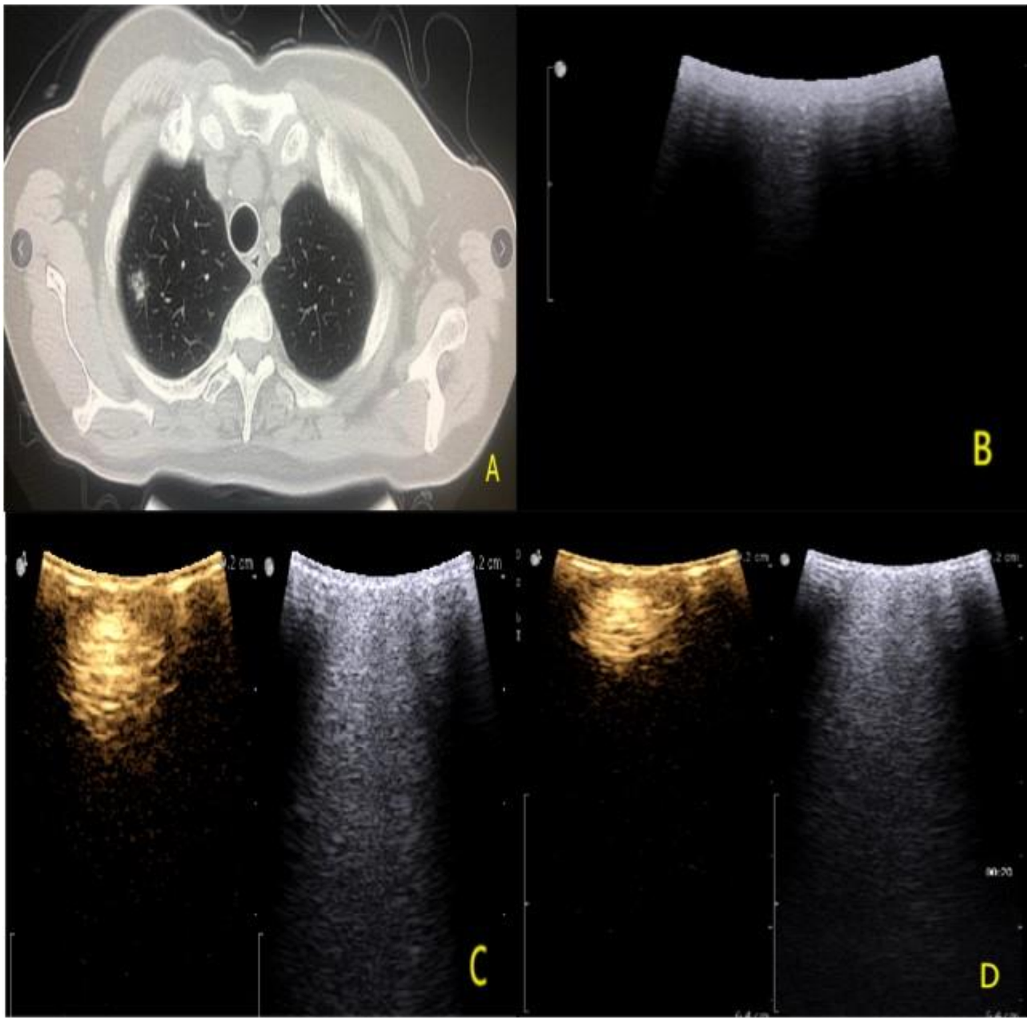

Figure 6. Preoperative HRCT, intraoperative ultrasonic and contrast-enhanced ultrasonic images of mGGN. A.Before operation, HRCT showed mGGN nodules about 13mm in diameter in the apical segment of the upper lobe of the right lung, with uneven density, irregular shape, spiny changes, lobulation sign and pleural indentation sign. B. The intraoperative two-dimensional ultrasonic showed that the echo in the nodule was uniform, hyperechoic, the boundary was not clear and the shape was regular. C, D. Intraoperative CEUS showed that the nodules began to enhance in 9 seconds, reached

the peak in 20 seconds, enhanced from the periphery to the center, and then disappeared rapidly, showing the appearance of “fast in and fast out”. HRCT: high resolution computed tomography; mGGN: partial ground glass nodule; CEUS: contrast-enhanced ultrasonic.

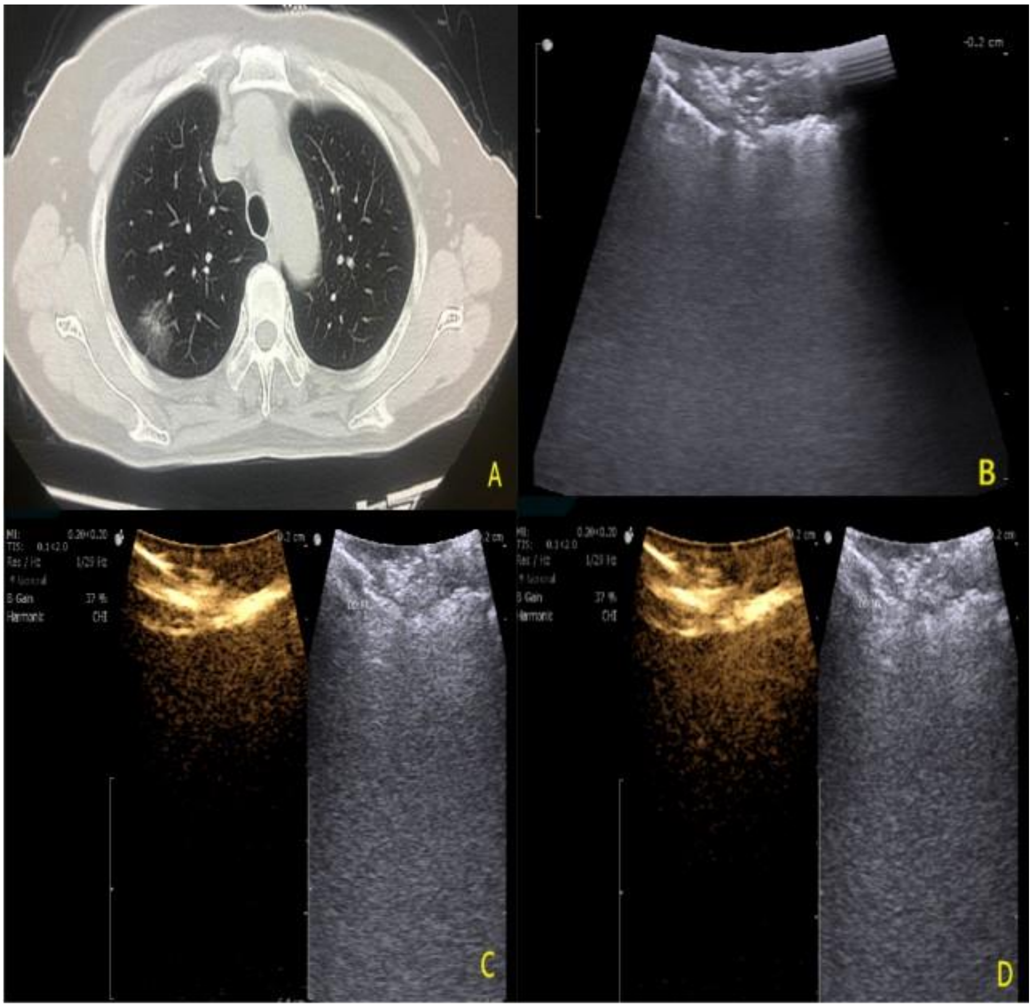

Figure 7. Preoperative HRCT, intraoperative ultrasonic and intraoperative contrast imaging of mGGN in the upper lobe of the right lung. A. Before operation, HRCT showed mGGN nodules with 22mm in diameter in the posterior segment of the upper lobe of the right lung, with uneven density, irregular shape, spiny changes, lobulation sign, pleural traction or depression sign. B. Intraoperative two-dimensional ultrasonic showed that mixed echoes were found in the nodules, mainly hypoechoic changes, unclear boundary and irregular shape. C, D. Intraoperative CEUS showed that the nodules began to enhance in 11 seconds, reached the peak in 16 seconds, and the nodular enhancement was mainly marginal enhancement, and then disappeared rapidly,

showing a “slow in and fast out” appearance. HRCT: high resolution computed tomography; mGGN: partial ground glass nodule; CEUS: contrast-enhanced ultrasonic.

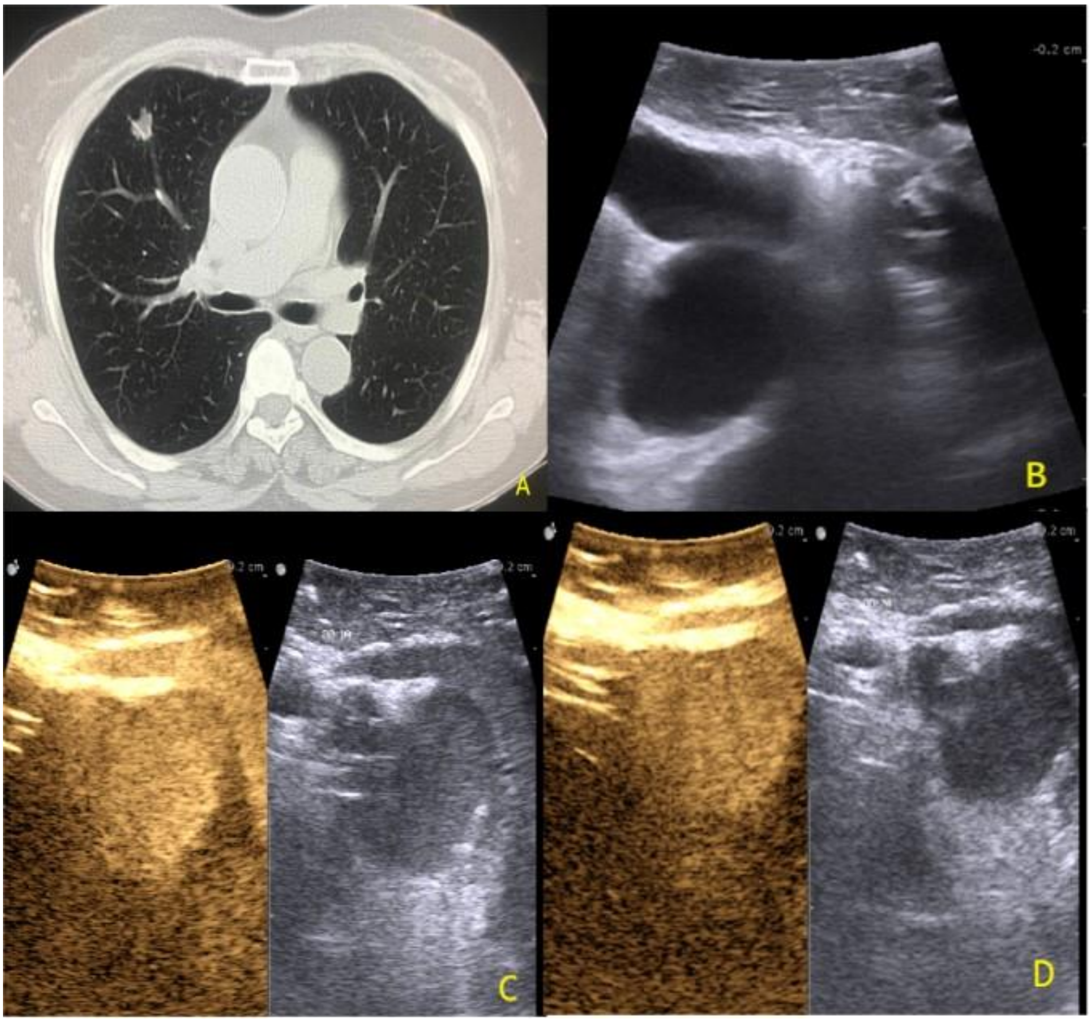

Figure 8. Preoperative HRCT, intraoperative ultrasonic and intraoperative contrast imaging of mGGN in the upper lobe of the right lung. A. Before operation, HRCT showed mGGN with 12mm in diameter in the anterior segment of the upper lobe of the right lung, with uneven density, irregular shape, spiny changes, shallow lobulation, and no signs of pleural traction or depression. B. Intraoperative two-dimensional ultrasonic showed that the echo of the nodule was uniform, hypoechoic, unclear boundary and irregular shape. C, D. During the operation, CEUS showed that the nodules began to enhance in 10 seconds, reached the peak in 24 seconds, enhanced from the periphery to the center, and then disappeared rapidly, showing the appearance of “slow in and fast out”. HRCT: high resolution computed tomography; mGGN: partial ground glass nodule; CEUS: contrast-enhanced ultrasonic.

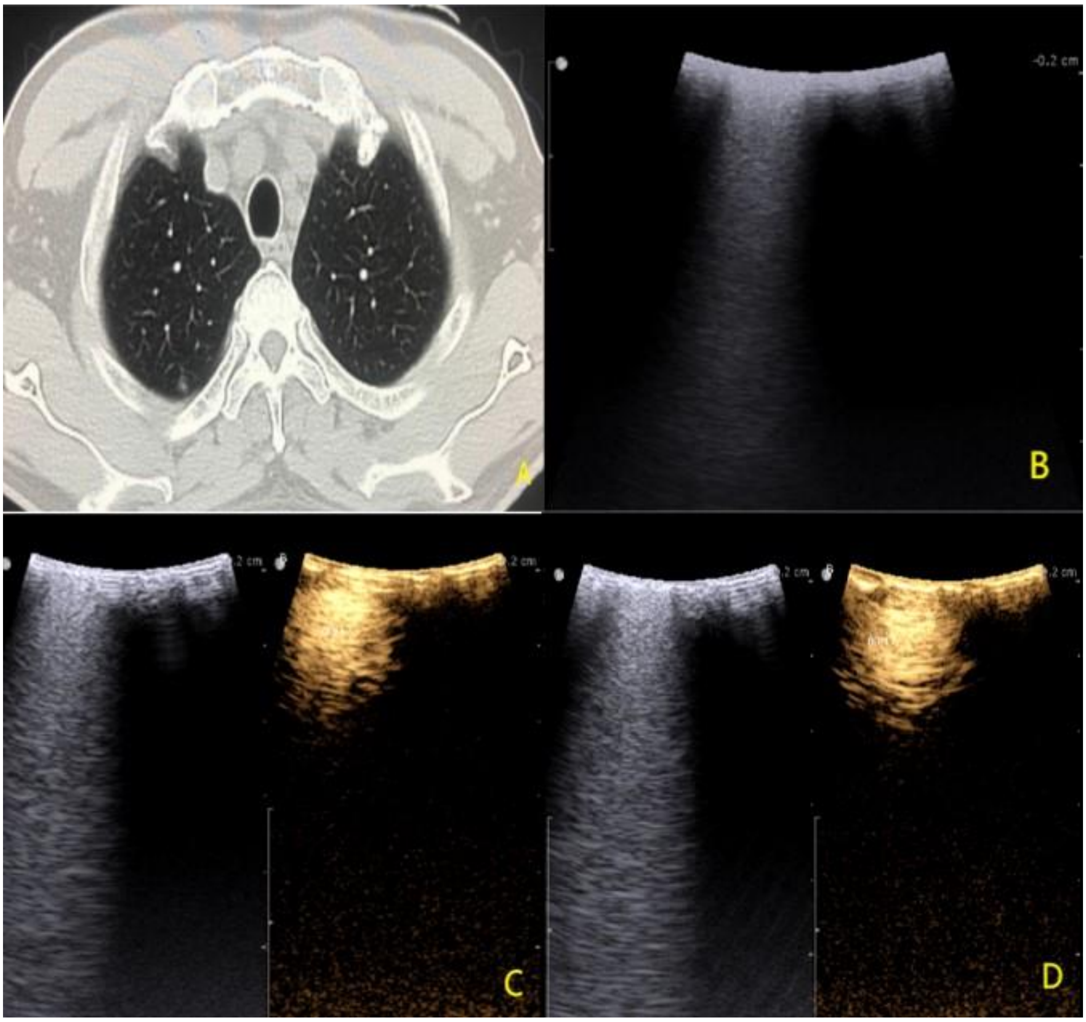

Figure 9. Preoperative HRCT, intraoperative ultrasonic and intraoperative contrast imaging of pGGN in the upper lobe of the right lung. A. Before operation, HRCT showed pGGN with 9mm in diameter in the posterior segment of the upper lobe of the right lung, with uniform density, regular shape, smooth edge, no lobulated changes, no burr-like changes, and no signs of pleural traction or depression. B. Intraoperative two-dimensional ultrasonic showed that the nodule had uniform echo, low echo, unclear boundary and regular shape. C, D. During the operation, CEUS showed that the nodules began to enhance in 12 seconds, reached the peak in 17 seconds, enhanced from the center to the periphery, and then disappeared rapidly, showing a "slow in and fast out" appearance. HRCT: high resolution computed tomography; pGGN: pure ground glass nodule; CEUS: contrast-enhanced ultrasonic.

DISCUSSION

Lung cancer is one of the malignant diseases with the highest morbidity and mortality in the world, which seriously threatens people's health and safety. In recent years, with the deepening of tumor screening awareness and the progress of CT technology, the detection rate of micro-lung cancer is increasing day by day. Clinically, micro-lung cancer often presents as pulmonary nodules on CT. In 2017, the Fleischner guidelines defined nodules as round-like opaque shadows with a diameter smaller than 3cm in the pulmonary parenchyma.[15] According to the number of solid components in the nodules, they can be divided into solid nodules and subsolid nodules, in which subsolid nodules can be divided into pGGN and mGGN. It has been reported that 20% pGGN and 40% mGGN will gradually show an increasing trend of solid composition,[16] and the continuous growth of solid composition of GGN is one of the malignant signs of small lung cancer. Surgical resection is the most effective method for the treatment of GGN. video-assisted thoracoscopic surgery (VATS) as a minimally invasive lung surgery method, compared with traditional thoracotomy, can greatly reduce postoperative pain and complications, and enable patients to recover earlier. However, in the treatment of pulmonary GGN lesions, how to accurately find and locate nodules according to various signs including intraoperative ultrasonic, preoperative CT and intraoperative palpation during VATS surgery is undoubtedly one of the difficult problems in front of chest doctors.

Since the beginning of this century, CT diagnosis of GGN lesions has increasingly become a hot topic in radiation medicine. According to the classification, diameter, edge, density and other characteristics of GGN, HRCT has been able to make a more accurate diagnosis of GGN lesions.[17] In the field of ultrasonic diagnosis, although Santambrogio *et al.* proposed that intraoperative ultrasonic can safely and effectively locate pulmonary nodules during video-assisted thoracoscopic surgery,[10] there is still a lack of systematic research on intraoperative ultrasonic detection and localization of GGN lesions on CT. At the same time, the study of intraoperative ultrasonographic signs of vats, which can be adopted for the detection and localization of GNN lesions, is more rare. In view of this, this study summarized the intraoperative two-dimensional ultrasonic and contrast-enhanced ultrasonic features of small lung cancer lesions with ground glass nodules on CT.

Comparison of HRCT and vats intraoperative ultrasonographic features of ground glass nodules of the lung

On the CT images of the lung, ground glass shadow refers to the irregular translucent density area with unclear or blurred boundary in the lung. In this area, the texture of the blood vessels and bronchial walls is still clearly visible. In addition to inflammatory lesions, bleeding and other non-neoplastic lesions, ground glass nodules can also be shown in peripheral lung adenocarcinoma, bronchiolar alveolar carcinoma, atypical adenomatous hyperplasia, lymphoma and other lesions.[18] Although GGN is a non-specific imaging feature, pathological types include partial exudation of lung tissue, tumor cell infiltration, interstitial inflammatory thickening, fibrosis, edema and so on, peripheral lung cancer characterized by GGN often shows unique signs of malignant tumor on CT, such as marginal spiculation sign, lobulation sign, pleural indentation sign, air bronchus sign and so on.[19] In the micro-lung cancer in this study, the positive rates of marginal spiculation sign, lobulation sign and pleural indentation sign were 68.18%, 47.72% and 56.81%, respectively. It indicates that the above signs are still important signs of micro-lung cancer characterized by GGN, which is consistent with the results of Zheng.[20]

In VATS surgery, ultrasonic detects and locates pulmonary nodules, especially GGN, through the collapsed lung tissue, and it is often necessary to observe the sonographic features of the detected nodules. In previous operations for hepatobiliary tumors, the short diameter of the lesion on CT or MRI before operation is often adopted as the basis for finding the lesion.[21] However, this study shows that there is a significant difference in the short diameter of GGN lung cancer lesions between HRCT and intraoperative ultrasonic images ($P < 0.05$), that is, the same ground glass nodule lung cancer lesions are difficult to find, locate and accurately confirm during operation because of the difference in short diameters between HRCT and intraoperative ultrasonic images. Throughout the literature, the author believes that there are still some normal or abnormal gas-containing structures communicating with bronchioles in GGN lung cancer, and the measurement diameter of GGN lung cancer can be reduced due to the excretion of gas components along the bronchioles in the state of lung collapse.

Although the burr sign and pleural indentation sign based on the density difference between the lesion and the surrounding lung tissue and pleural tissue can not be well observed on CT images due to the collapse of lung tissue, but the shape and edge of the lesion can still be well displayed. In this study, the morphological and marginal differences of GGN lung cancer lesions on HRCT and intraoperative ultrasonic images were studied. The results showed that there was no significant difference in morphology and edge between the two images ($P > 0.05$). As a consequence, we believe that in VATS surgery, the operator should be based on the shape and edge characteristics of the lesions on the preoperative CT, and can identify the lesions observed by ultrasonic, rather than by comparing the size of the lesions on the CT before operation.

Comparison of intraoperative ultrasonographic features of pure ground glass nodule lung cancer and partial solid ground glass nodule lung cancer

Although both pGGN and mGGN are important manifestations of subsolid nodules on CT, mGGN lung cancer tends to be less differentiated and more aggressive than pGGN lung cancer of similar size.[22] In vats, intraoperative ultrasonic can be adopted to distinguish pGGN lung cancer from mGGN lung cancer, which also has certain clinical application value.

In this study, the average diameters of pGGN and mGGN were compared by CT images. the results showed that the average diameters of the two groups were 11.20 ± 3.96mm and 16.93 ± 5.40mm, respectively. The difference of average diameter between the two groups was statistically significant ($P < 0.05$). Accordingly, Fan *et al.* believe that the nodule size can reflect the differentiation of GGN to a certain extent, that is, the larger the nodule is, the higher the malignant degree may be; the smaller the nodule is, the more uniform the density is, the less likely it is to be malignant.[23] However, the comparative study of ultrasonography between pGGN lung cancer and mGGN lung cancer has not been reported.

This study showed that the intraoperative ultrasonic images of pGGN lung cancer and mGGN nodule lung cancer were significantly different in short diameter and edge, but there was no significant difference in lesion shape, internal echo and echo pattern, that is, mGGN lung cancer tended to have a longer short diameter than pGGN lung cancer, which was consistent with the results of Lee *et al*.[24] At the same time, the authors believe that mGGN lung cancer lesions tend to be lobulated compared with pGGN lung cancer lesions. Throughout the literature, the author believes that the differentiation of mGGN lung cancer is low, and the proliferation rate of each part is different, which may be the pathophysiological basis for the formation of lobulated margin.

Characteristics of intraoperative contrast-enhanced ultrasonography in lung cancer with ground glass nodules

With the progress and maturity of ultrasonic technology, intraoperative CEUS arises at the historic moment, and it increasingly plays its unique advantages in the intraoperative diagnosis and treatment of hepatobiliary tumors and other diseases.

However, up to now, the study on the characteristics of intraoperative CEUS in VATS for GGN lung cancer has not been reported. For this reason, 15 cases of GGN lung cancer were collected in this study. TE, TTP, enhancement mode, enhancement intensity and other characteristic indexes were observed by intraoperative CEUS in VATS, so as to lay a foundation for future large sample study.

This study showed that there was a significant difference in TE and TTP between GGN lung cancer lesions and collapsed lung tissues ($P < 0.05$), that is, GGN lung cancer lesions could be better demonstrated by CEUS in collapsed lung tissues, which was consistent with the conclusion of CEUS study of percutaneous transthoracic wall adhesion to pleural adhesion of peripheral lung cancer by Bi *et al*.[25] In view of the fact that the components of GGN lung cancer lesions may contain structures such as pulmonary vessels or bronchi, or the residual gas is similar to the echo of incomplete lung tissue,[26] it is difficult to show its boundary by conventional ultrasonic. Contrast-enhanced ultrasonic may be more effective in the diagnosis of GGN lung cancer lesions which are difficult to be detected and diagnosed during VATS.

This study showed that the enhancement mode and enhancement intensity of 15 cases of GGN lung cancer were mainly “slow in and fast out” mode and “low enhancement” mode respectively, accounting for more than 80%. Throughout the literature, the lung has the characteristics of dual blood supply, that is, the pulmonary artery and bronchial artery participate in the blood supply. The bronchial artery system mainly provides nutrition for bronchi, pulmonary vessels, alveoli, interstitial tissue and visceral pleura, while the pulmonary artery system is mainly responsible for gas exchange. Theoretically, GGN lung cancer lesions are mainly supplied by the bronchial artery system, and collapsed lung tissue is mainly supplied by the pulmonary artery system.[27] Some studies have shown that the time to peak of pulmonary artery blood supply during enhancement is earlier than that of bronchial artery blood supply,[28] so the lesions of GGN lung cancer which are mainly supplied by bronchial artery often show “slow in and fast out” mode. In addition, in the process of enhancement, the collapsed lung tissue was enhanced early because it was mainly supplied by the pulmonary artery system, so the small GGN lung cancer lesions showed “low echo” in contrast-enhanced ultrasonography. With the increase of bronchial artery blood supply, the lesions of GGN lung cancer were mostly small lung cancer, and the tumor abnormal vessels were not rich in infiltrative lung cancer, so the enhancement still showed “slight increase”, thus forming the overall manifestation of “low enhancement”.

Recently, the objective identification of pulmonary artery and bronchial artery blood supply of pulmonary lesions in the world has increasingly become the lesion of research. The latest guidelines of the European Association of Ultrasonic Medicine suggest that when the enhancement time of intrapulmonary lesions is less than 10 seconds, it indicates that pulmonary artery blood supply is dominant; when the enhancement time of pulmonary lesions is more than 10 seconds, it shows that bronchial artery blood supply is dominant.[29] However, some scholars believe that when the enhancement time of pulmonary lesions is less than 6 seconds, it is the blood supply period of pulmonary artery; when the enhancement time of pulmonary lesions is more than 6 seconds, it is the blood supply period of bronchial artery.[30] In this group, the initial enhancement time of GGN lung cancer lesions was mainly after 10 seconds, while that of collapsed lung tissue was mainly 10 seconds ago, which was consistent with the guidelines of the European Association of Ultrasonic Medicine.[29] As a consequence, the authors believe that the intraoperative contrast-enhanced ultrasonic time of GGN in pulmonary lesions can indicate the possible source of arterial blood supply, and it is also expected to become an important basis for intraoperative differentiation of VATS lesions.

Although this study has achieved some results, there are still some shortcomings: (1) This study only included 44 ground glass nodular lung cancer from a single center, and the sample size was small, especially the intraoperative contrast-enhanced ultrasonic in vats was only a summary of individual cases. it needs to be further verified by a large sample and multicenter systematic study in the future. (2) This study only collected the lung cancer lesions with GGN on CT, but did not include benign lesions, and failed to make a comparative study on the ultrasonographic features of benign and malignant lesions with ground glass nodules. (3) In the collection of imaging data, it was mainly observed by imaging doctors, and the model was not established by the combination of imaging and clinical data, so it was subjective.

CONCLUSION

The small lung cancer lesions with ground glass nodules on CT have certain imaging features on the intraoperative ultrasonic images of vats. Mastering these characteristics has a certain clinical value for the detection and diagnosis of lesions during VATS, and then to complete the accurate resection of these lesions. During the VATS operation of GGN lung cancer, the lesions observed by ultrasonic can be distinguished according to the shape and edge characteristics of the lesions on CT before operation. In terms of intraoperative ultrasonographic features of VATS, mGGN has a longer short diameter of lesions than pGGN, and the edge of lesions is more lobulated. Contrast-enhanced ultrasonic mostly showed low enhancement in GGN micro-lung cancer, and the contrast mode was “slow in and fast out”. The use of this feature is beneficial to the confirmation of micro-lung cancer nodules during operation.

Source of Funding

None declared.

Ethics Approval and Consent to Participate

Our study was approved by the Medical Ethical Committee of Liaoning Cancer Hospital and Institute (Number: 20210407X). All the patients were informed and consented to use their general characteristics and imaging data.

Conflict of Interest

None declared.

REFERENCES

1. Sung H, Ferlay J, Siegel RL, Laversanne M, Soerjomataram I, Jemal A, *et al*. Global Cancer Statistics 2020: GLOBOCAN Estimates of Incidence and Mortality Worldwide for 36 Cancers in 185 Countries. CA Cancer J Clin 2021;71:209–249.
2. Vlahos I, Stefanidis K, Sheard S, Nair A, Sayer C, Moser J. Lung cancer screening: nodule identification and characterization. Transl Lung Cancer Res 2018;7:288–303.
3. Shao SC, Cai Q, Tong MM, Chen Q, Zhao CH, Shen YY. Application of multi-slice spiral CT three-dimensional reconstruction in micro-lung cancer. J Clin Radiol 2021;40:267–270.
4. Thai AA, Solomon BJ, Sequist LV, Gainor JF, Heist RS. Lung cancer. Lancet 2021;398:535–554.
5. Soultanis KM, Chen Chao M, Chen J, Wu L, Yang C, Gonzalez-Rivas D, *et al*. Technique and outcomes of 79 consecutive uniportal video-assisted sleeve lobectomies. 2019;56:876–882.
6. Owan TE, Hodge DO, Herges RM, Jacobsen SJ, Roger VL, Redfield MM. Trends in prevalence and outcome of heart failure with preserved ejection fraction. N Engl J Med 2006;355:251–259.
7. Awais O, Reidy MR, Mehta K, Bianco V, Gooding WE, Schuchert MJ, *et al*. Electromagnetic Navigation Bronchoscopy-Guided Dye Marking for Thoracoscopic Resection of Pulmonary Nodules. Ann Thorac Surg 2016;102:223–229.
8. Deng C, Cao X, Wu D, Ding H, You R, Chen Q, *et al*. Small lung lesions invisible under fluoroscopy are located accurately by three-dimensional localization technique on chest wall surface and performed bronchoscopy procedures to increase diagnostic yields. BMC Pulm Med 2016;16:166.
9. Park CH, Han K, Hur J, Lee SM, Lee JW, Hwang SH, *et al*. Comparative Effectiveness and Safety of Preoperative Lung Localization for Pulmonary Nodules: A Systematic Review and Meta-analysis. Chest 2017;151:316–328.
10. Santambrogio R, Montorsi M, Bianchi P, Mantovani A, Ghelma F, Mezzetti M. Intraoperative ultrasonic during thoracoscopic procedures for solitary pulmonary nodules. Ann Thorac Surg 1999;68:218–222.
11. Ujiie H, Kato T, Hu HP, Hasan S, Patel P, Wada H, *et al*. Evaluation of a New ultrasonic Thoracoscope for Localization of Lung Nodules in Ex Vivo Human Lungs. Ann Thorac Surg 2017;103:926–934.
12. Piolanti M, Coppola F, Papa S, Pilotti V, Mattioli S, Gavelli G. Ultrasonographic

localization of occult pulmonary nodules during video-assisted thoracic surgery. Eur Radiol 2003;13:2358–2364.
13. Huang YH, Chen K C, Chen JS. Ultrasonic for intraoperative localization of lung nodules during thoracoscopic surgery. Ann Transl Med 2019;7:37.
14. Hou YL, Wang YD, Guo H Q, Zhang Y, Guo Y, Han H. Ultrasonic location of pulmonary nodules in video-assisted thoracoscopic surgery for precise sublobectomy. Thorac Cancer 2020;11:1354–1360.
15. Macmahon H, Naidich DP, Goo J M, Lee KS, Leung ANC, Mayo JR, *et al*. Guidelines for Management of Incidental Pulmonary Nodules Detected on CT Images: From the Fleischner Society 2017. Radiology 2017;284:228–243.
16. Kobayashi Y, Ambrogio C, Mitsudomi T. Ground-glass nodules of the lung in never-smokers and smokers: clinical and genetic insights. Transl Lung Cancer Res 2018;7:487–497.
17. Zhang P, Li T, Tao X, Jin X, Zhao S. HRCT features between lepidic-predominant type and other pathological subtypes in early-stage invasive pulmonary adenocarcinoma appearing as a ground-glass nodule. BMC Cancer, 2021;21:1124.
18. Lv YG, Bao JH, Xu DU, Yan QH, Li YJ, Yuan DL, *et al*. Characteristic analysis of pulmonary ground-glass lesions with the help of 64-slice CT technology. Eur Rev Med Pharmacol Sci 2017;21:3212–3217.
19. Jin X, Zhao SH, Gao J, Wang DJ, Wu J, Wu CC, *et al*. CT characteristics and pathological implications of early stage (T1N0M0) lung adenocarcinoma with pure ground-glass opacity. Eur Radiol 2015;25:2532–2540.
20. Zheng H, Zhang H, Wang S, Xiao F, Liao M. Invasive Prediction of Ground Glass Nodule Based on Clinical Characteristics and Radiomics Feature. Front Genet 2021;12:783391.
21. Russolillo N, Borello A, Langella S, Casella M, Lo Tesoriere R, Ferrero A. Comparison of laparoscopic ultrasonic and liver-specific magnetic resonance imaging for staging colorectal liver metastases. Surg Endosc 2021;35: 3547–3553.
22. Hattori A, Suzuki K, Takamochi K, Wakabayashi M, Aokage K, Saji H, *et al*. Prognostic impact of a ground-glass opacity component in clinical stage IA non-small cell lung cancer. J Thorac Cardiovasc Surg 2021;161:1469–1480.
23. Fan L, Liu SY, Li QC, Yu H, Xiao XS. Multidetector CT features of pulmonary focal ground-glass opacity: differences between benign and malignant. Br J Radiol 2012;85:897–904.

24. Lee HJ, Kim YT, Kang CH, Zhao B, Tan Y, Schwartz LH, *et al*. Epidermal growth factor receptor mutation in lung adenocarcinomas: relationship with CT characteristics and histologic subtypes. Radiology 2013;268:254–264.

25. Bi K, Zhou RR, Zhang Y, Shen MJ, Chen HW, Cong Y, *et al*. US Contrast Agent Arrival Time Difference Ratio for Benign versus Malignant Subpleural Pulmonary Lesions. Radiology 2021;301:200–210.

26. Zhang Y, Fu F, Chen H. Management of Ground-Glass Opacities in the Lung Cancer Spectrum. Ann Thorac Surg 2020;110:1796–1804.

27. Sartori S, Postorivo S, Vece FD, Ermili F, Tassinari D, Tombesi P. Contrast-enhanced ultrasonography in peripheral lung consolidations: What's its actual role? World J Radiol 2013;5:372–380.

28. Linde HN, Holland A, Greene BH, Görg C. [Contrast-enhanced sonography (CEUS) in pneumonia: typical patterns and clinical value - a retrospective study on *n* = 50 patients]. Ultraschall Med 2012;33:146–151.

29. Sidhu PS, Cantisani V, Dietrich CF, Gilja OH, Saftoiu A, Bartels E, *et al*. The EFSUMB Guidelines and Recommendations for the Clinical Practice of Contrast-Enhanced ultrasonic (CEUS) in Non-Hepatic Applications: Update 2017 (Long Version). Ultraschall Med 2018;39:2–44.

30. Görg C, Bert T, Kring R, Dempfle A. Transcutaneous contrast enhanced sonography of the chest for evaluation of pleural based pulmonary lesions: experience in 137 patients. Ultraschall Med 2006;27:437–444.